

## Does Rotation Influence Double-Diffusive Fluxes in Polar Oceans?

J. R. CARPENTER AND M.-L. TIMMERMANS

*Department of Geology and Geophysics, Yale University, New Haven, Connecticut*

(Manuscript received 2 May 2013, in final form 23 September 2013)

### ABSTRACT

The diffusive (or semiconvection) regime of double-diffusive convection (DDC) is widespread in the polar oceans, generating “staircases” consisting of high-gradient interfaces of temperature and salinity separated by convectively mixed layers. Using two-dimensional direct numerical simulations, support is provided for a previous theory that rotation can influence DDC heat fluxes when the thickness of the thermal interface sufficiently exceeds that of the Ekman layer. This study finds, therefore, that the earth’s rotation places constraints on small-scale vertical heat fluxes through double-diffusive layers. This leads to departures from laboratory-based parameterizations that can significantly change estimates of Arctic Ocean heat fluxes in certain regions, although most of the upper Arctic Ocean thermocline is not expected to be dominated by rotation.

### 1. Introduction

The thermohaline structure of polar oceans is known to produce regions of double-diffusive convection (DDC) (Schmitt 1994; Kelley et al. 2003). The convection is almost exclusively of the diffusive type with cool, fresh waters overlying warmer, saltier waters. Such conditions are often found to exhibit a double-diffusive staircase in which the water column forms a series of homogeneous mixed layers where small-scale convective mixing is taking place, separated by relatively thinner density-stratified interfaces (Fig. 1). We shall restrict ourselves to the diffusive regime, where the heat fluxes that result from DDC have been suggested to be an important contribution to the upper-ocean heat budget of the Arctic Ocean (e.g., Polyakov et al. 2012; Turner 2010). DDC is widespread throughout the Arctic Ocean, and many different staircase properties have been observed. For example, temperature interface thicknesses  $h$  have been reported to have a range of  $0.05 \leq h \leq 20$  m, with jumps in temperature of  $0.001 \leq \Delta T \leq 0.5^\circ\text{C}$ , leading to heat flux estimates of  $0.02 \leq F_H \leq 10 \text{ W m}^{-2}$  (Padman and Dillon 1987, 1989; Timmermans et al. 2003, 2008; Polyakov et al. 2012; Carmack et al. 2012; Sirevaag and Fer 2012). Despite this large variability, oceanic DDC heat flux estimates are

often based on the application of laboratory-derived laws (e.g., Marmorino and Caldwell 1976; Kelley 1990), and it is unclear whether oceanic conditions are appropriately parameterized by these laws in all cases.

In this paper, we demonstrate that planetary rotation can cause much-reduced heat fluxes that would otherwise result from applying the laboratory-based DDC parameterizations. At first suggestion, the influence of planetary rotation on small-scale convective fluxes might seem surprising, as rotational effects are usually thought important over large length and time scales, coincident with a balance between buoyancy and Coriolis forces. However, it has been argued that the relevant control on thermal convection systems is governed by rotational effects within thin thermal boundary layers (Kelley 1987; King et al. 2009). The transition between nonrotating and rotationally dominated heat transfer is then determined by the relative thickness of the Ekman and thermal boundary layers; when the Ekman layer is small relative to the thermal boundary layer, rotation will modify the heat transfer within the boundary layers that supply turbulent convection in the bulk.

In DDC, temperature interfaces will produce frictional Ekman layers with a vertical scale on the order of the Ekman length  $\delta_E \equiv (\nu/f)^{1/2}$ , where  $\nu$  is the kinematic viscosity, and  $f$  is the Coriolis parameter. If the interfaces are assumed to be laminar, it is possible to draw an analogy between the temperature interface in DDC and the thermal boundary layer of thermal convection. In this case, a condition originally developed by Kelley

---

*Corresponding author address:* Jeff Carpenter, Institute for Coastal Research, Helmholtz Zentrum Geesthacht, Max-Planck-Strasse 1, Geesthacht 21502, Germany.  
E-mail: jeff.carpenter@hzg.de

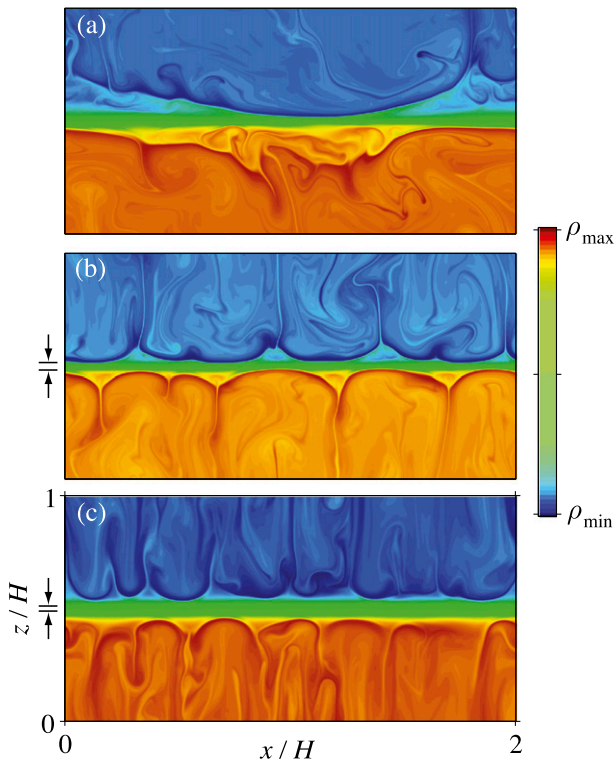


FIG. 1. Representative density fields from the high-Rayleigh number simulations ( $Ra = 1.6 \times 10^7$ ) with density ratio  $R_\rho = 5$  at increasing rotation rates with (a) no rotation, (b) Ekman number  $Ek = 2.5 \times 10^{-4}$ , and (c)  $Ek = 8.3 \times 10^{-5}$ . The Ekman layer thickness is shown as the scale on the left with (b) rotation rate  $H/\delta_E = 33$  and (c)  $H/\delta_E = 55$ . Note the nonlinear color scale used to visualize the mixed layers and boundary layers.

(1987), based on data from the thermal convection experiments of Rossby (1969), predicts a transition to rotationally dominated heat fluxes will occur when  $h > B\delta_E$ , where  $B = 5.6$  is an empirical constant.<sup>1</sup> Because polar oceans are characterized by  $11 < \delta_E < 12$  cm (i.e.,  $63 < B\delta_E < 67$  cm), for latitudes higher than  $60^\circ$ , it is not surprising that rotation may influence DDC heat fluxes in some cases. In this paper, we provide the first test of the Kelley (1987) theory by using a series of direct numerical simulations. The results are then used to determine regions where rotation is expected to play a significant role in DDC heat transport.

## 2. Simulations

The direct numerical simulations (DNS) are performed using the code described by Winters et al. (2004), and simulate a two-dimensional incompressible Boussinesq

fluid using a linear equation of state for the density contribution of the temperature  $T$  and salinity  $S$  scalars [see Carpenter et al. (2012a) and Flanagan et al. (2013) for a discussion on DNS of diffusive convection]. Periodic boundary conditions are used on all boundaries except with mean jumps of  $T$  and  $S$  restored when fluid parcels cross the top and bottom boundaries (i.e., the  $T$  and  $S$  anomalies with respect to a reference profile are periodic in the vertical). Therefore, the mean  $T$  and  $S$  differences across the interface remain approximately constant during the simulation, and the basic configuration consists of a single double-diffusive interface with an identical mixed layer on either side that is within an infinitely deep staircase in a rotating frame of reference.

Of primary interest is the flux of heat across this interface, given some external measurable properties. The problem may be formulated in terms of the dimensionless heat flux  $Nu \equiv F_H H / \rho c_p \kappa_T \Delta T$ , called the Nusselt number, which will be determined by the following dimensionless parameters describing a single mixed layer and interface: (i) the Rayleigh number  $Ra \equiv g\alpha\Delta TH^3 / \nu\kappa_T$  quantifying the thermal forcing, (ii) the Ekman number  $Ek \equiv \nu / fH^2 = \delta_E^2 / H^2$  expressing the importance of rotation through the relative thickness of the Ekman layer, and (iii) the density ratio  $R_\rho \equiv \beta\Delta S / \alpha\Delta T$  giving the relative buoyancy contributions of  $T$  and  $S$  across the interface. In addition to the above parameters, we can also define (iv) the Prandtl number  $Pr \equiv \nu / \kappa_T$ , and (v) the diffusivity ratio  $\tau \equiv \kappa_S / \kappa_T$ , which are both properties of the ocean water column. The dimensional scales used above are the water density  $\rho$ ; the heat capacity  $c_p$ ; the gravitational acceleration  $g$ ; the thermal expansion and saline contraction coefficients  $\alpha$  and  $\beta$ , respectively; the jumps of temperature and salinity across the interface  $\Delta T$  and  $\Delta S$ , respectively; the depth of a single mixed layer and interface  $H$ ; and the molecular diffusion coefficients of temperature and salinity  $\kappa_T$  and  $\kappa_S$ , respectively.

The heat flux is calculated directly from the following definition [see Winters and D'Asaro (1996) for details]

$$F_H \equiv \frac{\rho c_p}{A} \int_\sigma \kappa_T \nabla T \cdot \hat{\mathbf{n}} d\sigma = \frac{\rho c_p}{A} \int_\sigma \kappa_T |\nabla T| d\sigma, \quad (1)$$

where  $\hat{\mathbf{n}}$  is the unit vector normal to the surface of integration  $\sigma$ , taken as the central isotherm of the interface, and  $A$  is the plane cross-sectional area (i.e., not the area of the  $\sigma$  surface). The second equality follows because  $\sigma$  is an isothermal surface. In the case of a two-dimensional domain, the surface integral reduces to a line integral and  $F_H$  is expressed per unit width. The  $F_H$  obtained in this way were compared to the advective flux given by

$$F_H^{\text{adv}} \equiv -\rho c_p \langle wT \rangle_A, \quad (2)$$

<sup>1</sup>This form was never explicitly stated in Kelley (1987) but follows directly from his analysis.

where  $w$  is the vertical velocity, and  $\langle \cdot \rangle_A$  indicates a spatial average over a plane area  $A$  that is taken in the center of the mixed layer. Time-averaged estimates of  $F_H$  were found to agree to within 2% of  $F_H^{\text{adv}}$  on average for the simulations that reach a steady state. Large fluctuations in time were found in  $F_H^{\text{adv}}$ , resulting in a dependence on the averaging period, which caused these differences. We therefore use the  $F_H$  computed from (1) throughout.

The simulations are initiated by prescribing each of the five dimensionless numbers above together with an initial interface thickness  $h_0$ . For the majority of the simulations we fix  $H/h_0 = 11$ , but in one sequence  $H/h_0$  is varied. A random perturbation is applied to the vertical velocity field at the initial time step in order to seed the instabilities that develop near the interface (Carpenter et al. 2012b). Because we are interested in determining the condition that controls the transition to a rotation-dominated heat flux, we have fixed  $\text{Pr} = 6.25$  and  $\tau = 0.01$ , but vary  $R_\rho$ ,  $\text{Ra}$ , and  $\text{Ek}$ . Polar oceans typically have  $\text{Pr} \approx 13$  and  $\tau \approx 0.005$ , and this difference should have an effect on  $F_H$ , however, it is not expected to change the condition that determines the importance of rotation on  $F_H$ . This is supported by the rotating thermal convection simulations of King et al. (2009), who show that this condition is independent of  $\text{Pr}$ . The simulated values of  $\text{Pr}$  and  $\tau$  are, however, characteristic of the DDC staircase in tropical Lake Kivu (Schmid et al. 2010; Carpenter et al. 2012a; Sommer et al. 2013b) and representative of subtropical regions.

Simulating low values of  $\tau$  places especially large constraints on the computational grid and the size of the domain. This is due to the small scales that result from the slow diffusion of  $S$ . The Batchelor scale  $L_B$  is often used as a measure of the smallest scales that result from the advection and diffusion of a scalar quantity in a flow. It is expressed in terms of the volume-averaged rate of kinetic energy dissipation  $\epsilon$ , as  $L_B \equiv (\nu\kappa_S^2/\epsilon)^{1/4}$  for the  $S$  field. Despite well-resolved DNS at grid spacings  $\Delta x$  that are as large as  $2.5L_B$  in stably stratified mixing layers, Carpenter et al. (2012a) have found that diffusive convection requires  $\Delta x/L_B \lesssim 2$ . In the present simulations, the largest  $\Delta x/L_B$  ratio at steady state was 1.23. Flanagan et al. (2013) have suggested a different criteria based on the length scale  $\ell \equiv (\kappa_T\nu/g\alpha\Delta T)^{1/4}$ . They found that DNS of diffusive convection was well resolved when  $\Delta x$  was comparable to  $\ell\tau^{1/2}$ , and the largest value found in our simulations is  $\Delta x/\ell\tau^{1/2} = 0.82$ .

In all simulations, the aspect ratio is fixed with the horizontal domain size twice that in the vertical (Fig. 1). Nine different values of  $\text{Ek}$  were simulated, beginning with the nonrotating case of infinite  $\text{Ek}$ , and spaced approximately logarithmically to the strongest rotation at  $\text{Ek} = 2.5 \times 10^{-5}$ . Because  $\text{Nu}$  is expected to be dependent

on  $\text{Ra}$  (Turner 1965), three values of  $\text{Ra}$  ( $6.5 \times 10^5$ ,  $3.3 \times 10^6$ , and  $1.6 \times 10^7$ ) were simulated on evenly spaced grids of  $2048 \times 1024$  for the highest  $\text{Ra}$ , and  $1024 \times 512$  for the two lower- $\text{Ra}$  simulations. These simulations have all been conducted for a fixed  $R_\rho = 5$ . However, an additional sequence of simulations at relatively low  $R_\rho = 2$  and  $\text{Ra} = 3.3 \times 10^6$  have also been performed using the fine-grid spacing. In dimensional terms, the simulations correspond to scales relevant to oceanic DDC of  $H = 33$  cm and  $\Delta T = 1, 5$ , and  $24$  m °C at  $24^\circ\text{C}$  with a grid spacing of  $0.32$  and  $0.64$  mm. The  $F_H$  observed in the simulations reach values ( $\sim 0.4$  W m $^{-2}$ ) that are similar to those observed in both the Canada Basin thermocline (Padman and Dillon 1987; Timmermans et al. 2008) and in Lake Kivu (Sommer et al. 2013a,b).

The ability of 2D DNS to accurately capture the heat fluxes that are present in the equivalent 3D simulations was previously demonstrated by Carpenter et al. (2012a) and recently by Flanagan et al. (2013). Carpenter et al. (2012a) also show that the interface structure is accurately captured with 2D simulations. However, the agreement was only found for  $R_\rho \gtrsim 3$ . For this reason, the value of the heat flux in the  $R_\rho = 2$  simulations could be different than for an equivalent 3D simulation. Nonetheless, the results of the  $R_\rho = 2$  simulation are found to agree with the theory, and offer insight into the physics of double-diffusive convection.

### 3. Results and discussion

The effects of rotation on DDC can be seen qualitatively in the density fields shown in Fig. 1. In all cases, the interface acts as a source of buoyancy (and potential energy) for the convective motions in the mixed layer through the continual formation of small-scale buoyant plumes. These plumes originate from a convective instability of the gravitationally unstable diffusive boundary layer that results from the more rapid diffusion of the  $T$  interface relative to the  $S$  interface (Carpenter et al. 2012b). In the nonrotating and weakly rotating simulations, the mixed layer is found to develop a large-scale circulation that sweeps up the smaller-scale convective plumes together (Fig. 1a). As the rotation rate is increased this large-scale circulation cell is no longer present, and the horizontal spacing of the plumes is found to decrease (Figs. 1b,c). Flow in the mixed layer is increasingly dominated by the tendency of rotating convection to form tall, thin, columns in which the motion is primarily vertical (King et al. 2009). In addition, at relatively large rotation rates, the plumes are seen to oscillate horizontally close to the inertial frequency.

At low rotation rates, the presence of a single large-scale convection cell may indicate that the aspect ratio

will have an effect on the flow. This is generally the case when the cells that form are of a comparable size to the computational domain. At rotation rates that approach the transition, however, the presence of many cells in the domain (as seen in Figs. 1b,c) indicates that the domain size has minimal influence on the convective motions that develop. We therefore do not expect that the aspect ratio will affect our predictions of the transition to rotation-dominated heat fluxes in diffusive convection.

It is thought that for  $R_\rho \gtrsim 2$ , the central core of a diffusive interface is undisturbed from the mixed layer convection, and the heat fluxes can be well approximated by molecular conduction in the vertical, that is,

$$F_H^{\text{mol}} \equiv \rho c_p \kappa_T \langle \Delta T / h \rangle_\sigma, \quad (3)$$

where  $h \equiv \Delta T / (\partial T / \partial z|_\sigma)$  (Linden and Shirtcliffe 1978; Carpenter et al. 2012a), and the angled brackets indicate an average over the central isotherm as in (1). In this case, we can approximate  $\text{Nu} \approx H/h$ , and the condition determining the transition to rotation-dominated heat fluxes can be written in a general form as

$$\text{Nu}_t = C \text{Ek}^{-1/2}, \quad (4)$$

where  $\text{Nu}_t$  is the transition Nusselt number, and  $C = B^{-1} = 0.18$  is a constant (Kelley 1987; King et al. 2009). For  $\text{Nu} < \text{Nu}_t$ , rotation is expected to significantly reduce heat fluxes. We shall refer to (4) as the Kelley condition after Kelley (1987). An important assumption of the Kelley condition is that the heat flux through the interface is close to molecular, that is, that  $F_H \approx F_H^{\text{mol}}$ . The validity of this assumption is dependent on the value of  $R_\rho$  and is expected to breakdown at low  $R_\rho$ . Values of  $R_\rho$  in Arctic Ocean staircase interfaces are generally observed to be in the range  $1.4 \lesssim R_\rho \lesssim 6$  (Padman and Dillon 1987; Timmermans et al. 2003, 2008; Polyakov et al. 2012; Sirevaag and Fer 2012), and the present simulations are performed for  $R_\rho = 2$  and 5.

We test the Kelley condition by gradually increasing the rotation rate (measured by  $\text{Ek}^{-1/2} = H/\delta_E$ ) and calculate  $\text{Nu}$  to determine the transition from nonrotating to rotation-dominated heat fluxes (Fig. 2). The simulations can be divided into three different types indicated by the different symbols in Fig. 2. The first type is those at low rotation rates that reach a steady-state value of  $\text{Nu}$  (solid circles). This steady state follows after an initial period in which convection is initiated through instability of the “diffusive” boundary layers on the edges of the interface (Carpenter et al. 2012b). For low rotation rates, there is very little change in  $\text{Nu}$  from the nonrotating values at  $\text{Ek}^{-1/2} = 0$ . As the rotation rate

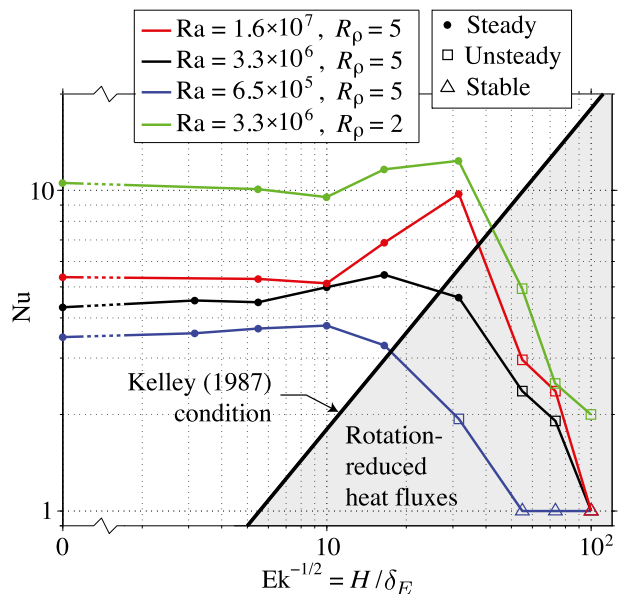


FIG. 2. Dimensionless heat flux ( $\text{Nu}$ ) versus  $\text{Ek}^{-1/2} = H/\delta_E$  for a series of simulations at different  $\text{Ra}$ . Solid circles indicate simulations that have reached a steady state, whereas hollow squares indicate that a steady state has not been reached, and therefore represents an upper bound on  $\text{Nu}$  for these particular simulations. Gray represents the region of parameter space in which the fluxes are expected to be strongly influenced by rotation, with the thick black line denoting the Kelley condition. For all simulations,  $H/h_0 = 11$ .

is increased and the simulations approach the Kelley condition,  $\text{Nu}$  is found to increase above the nonrotating values. This phenomenon is also observed in rotating thermal convection and has been explained by an enhanced vertical Ekman pumping velocity within the thermal boundary layer (Kunnen et al. 2006). An example of the density field in this regime is shown in Fig. 1b.

Once the rotation rate is increased further and the Kelley condition is crossed, the  $\text{Nu}$  drops as rotation strongly decreases heat fluxes. This finding parallels similar results in rotating thermal convection (Rossby 1969; King et al. 2009) and in salt finger convection (Schmitt and Lambert 1979). In these simulations (denoted by the hollow squares in Fig. 2) the  $\text{Nu}$  was not found to reach a steady state over the integration period. At the end of these simulations the  $T$  and  $S$  interfaces are still growing in thickness, and the  $\text{Nu}$  shown in Fig. 2 therefore represents only an upper bound for each simulation. An example of the density field for the high  $\text{Ra}$  simulation in this rotation-dominated regime is shown in Fig. 1c. It should be noted that for the two lower  $\text{Ra}$  simulations the convection in this regime was extremely ordered and cannot be called turbulent. Further increases in the rotation rate were found to completely stabilize the instability of the boundary layers, preventing convection from taking place (Fig. 2, triangles), and this takes place

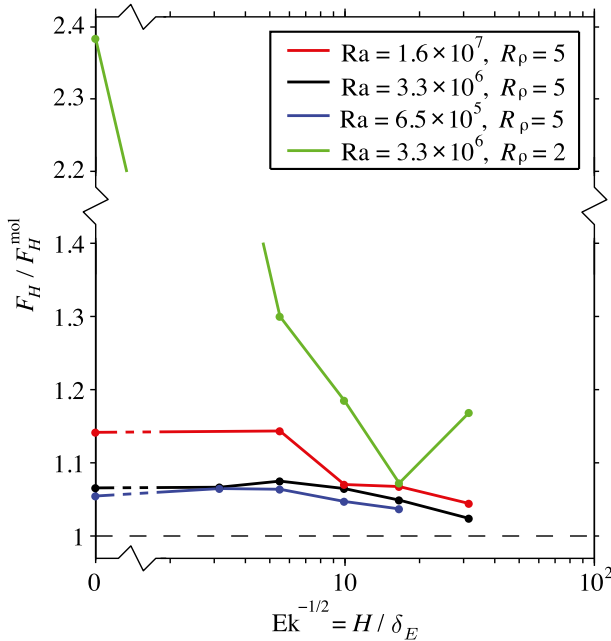


FIG. 3. The  $F_H/F_H^{\text{mol}}$  ratio for all simulations that reach a steady state. The plot has been “broken” to fit the large value of the nonrotating, low- $R_\rho$  simulation.

at relatively lower  $\text{Ek}^{-1/2}$  at lower Ra. A Nu of unity is found in these simulations corresponding to a motionless, purely conductive heat transfer.

Most of the simulations in the rotation-dominated regime have not reached a steady state by the end of the simulation because of the long integration times required for the slow thickening of the  $S$  interface by molecular diffusion. It is possible that these simulations eventually reach an Nu of unity, in which case the transition would not be resolved by our simulations. However, drawing an analogy with rotating thermal convection, we expect that steady-state interface thicknesses do exist close to the transition. The experiments of Rossby (1969) and simulations of King et al. (2009) demonstrate these steady states in rotating thermal convection. This is most likely not observed in our simulations because the resolution in Ek is not fine enough to resolve the relatively rapid drop in Nu. Therefore, we expect that it is possible for DDC staircases to exist that are governed by rotation-reduced heat fluxes.

The simulations can also be used to test the assumption of the Kelley condition that the fluxes through the interface are close to molecular. We do not expect that Kelley’s criterion holds when the flux through the interfaces is turbulent. In this case, the Ekman length must account for the turbulent exchange of momentum, which is usually accomplished by an increase in the viscosity above the molecular value. In Fig. 3, the  $F_H/F_H^{\text{mol}}$  ratio is

plotted as a function of the dimensionless rotation rate  $\text{Ek}^{-1/2}$ . It can be seen that the  $R_\rho = 5$  simulations are all within 15% of molecular fluxes, indicated by  $F_H/F_H^{\text{mol}} = 1$ . The general trend is for rotation to bring  $F_H$  closer to the molecular values. This is particularly evident in the low- $R_\rho$  simulations, where the nonrotating  $F_H/F_H^{\text{mol}} = 2.38$ , but close to the transition  $F_H$  is within 20% of  $F_H^{\text{mol}}$  (Fig. 3). This characteristic of rotating DDC to bring the interfacial heat fluxes close to molecular values ensures that the Kelley condition is valid even for low- $R_\rho$  interfaces that exhibit a significant “turbulent” heat transfer across them when rotation is not present. The Kelley condition, therefore, is able to predict the transition to a rotation-dominated  $F_H$  for the low  $R_\rho$  simulation, as is shown in Fig. 2.

All of the simulations used to construct Fig. 2 had the same initial interface thickness of  $H/h_0 = 11$ , and if  $\delta_E$  is sufficiently small we observe reduced  $\text{Nu} \approx H/h$ , and therefore thicker interfaces. An important question that we now address is whether it is possible to “push” an interface into the rotation-dominated regime by beginning with an initially thick interface. In Fig. 4, we choose four different  $H/h_0 = (2.5, 4.0, 8.0, 11)$  with all other parameters fixed, and plot the time evolution of a quantity that is approximately a normalized interface thickness, given by  $C\text{Nu}^{-1}\text{Ek}^{-1/2} \approx h/B\delta_E$ . This normalization is chosen so the Kelley condition corresponds to  $C\text{Nu}^{-1}\text{Ek}^{-1/2} = 1$ , with rotation-dominated fluxes expected above this level. The lowest (black) curve in Fig. 4 corresponds to the high-Ra simulation with the largest Nu in Fig. 2, with the density field shown in Fig. 1b. In each simulation there is an initial increase in interface thickness through molecular diffusion, with  $h(t) \propto (\kappa_T t)^{1/2}$ . This growth is reversed when the diffusive boundary layers break away from the interface and convection is initiated. In all but the largest  $h_0$  simulation, the convection is able to erode the interface toward the steady-state value observed in the  $H/h_0 = 11$  simulation (Fig. 2 and Fig. 4), which is not in the rotationally dominated regime. Although this steady state is not observed for the  $H/h_0 = 4.0$  simulation, it is assumed that it will eventually reach this state. For the  $H/h_0 = 2.5$  simulation, the convection is very weak, and it appears likely that it will remain in the rotationally dominated regime. Therefore, it is possible to push an interface into the rotation-dominated regime if the initial interface thickness is sufficiently large. In an oceanographic context, DDC interfaces may be thickened through some externally forced mixing event such as internal wave breaking or shear instability. Alternatively, it is possible for an interface to be pushed into the rotation-dominated regime, and then recover back to the nonrotating regime.

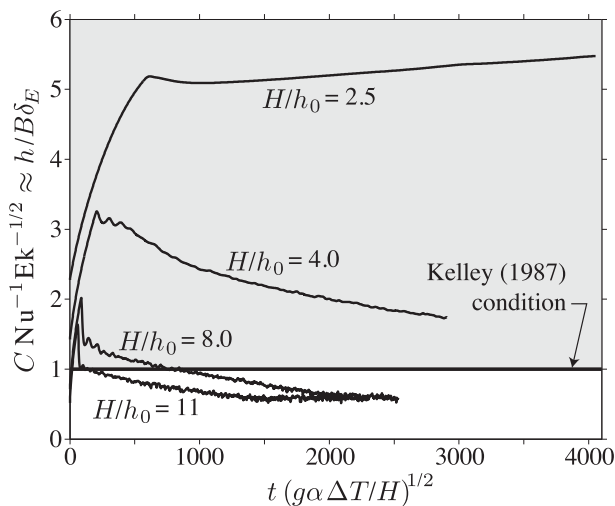


FIG. 4. Time evolution of  $C \text{Nu}^{-1} \text{Ek}^{-1/2}$ , which is approximately equivalent to the normalized interface thickness  $h(t)/B\delta_E$ . Each of the curves represents a simulation with a different  $h_0$  as shown. The time  $t$  has been nondimensionalized by the scale  $(H/g\alpha\Delta T)^{1/2}$ . As in Fig. 2, gray denotes the region of parameter space in which the fluxes are expected to be strongly influenced by rotation, with the Kelley condition shown by the black line. For all simulations  $\text{Ek}^{-1/2} = 33$ ,  $R_p = 5$ , and  $\text{Ra} = 1.6 \times 10^7$ . The  $H/h_0 = 11$  curve corresponds to the high-Ra simulation at  $\text{Nu} = 9.8$  in Fig. 2.

#### 4. Oceanic implications

Results of the DNS show support for the Kelley condition in determining the location of a rotation-induced transition to significantly reduced heat fluxes. Given this support, we can now address the question raised in the title of this paper, of whether rotation influences double-diffusive fluxes in polar oceans. This was previously discussed in Kelley (1987) using typical order-of-magnitude values from known double-diffusive staircases at that time, however, we revisit this question in light of recent observations of DDC in the Arctic Ocean.

A number of previous studies in polar regions have speculated on staircases in which the heat fluxes appear to be significantly less than the laboratory-derived laws (Howard et al. 2004; Timmermans et al. 2003; Polyakov et al. 2012; Carmack et al. 2012). A number of mechanisms may be important for the observed flux reduction, such as a mean shear present across the interfaces (Polyakov et al. 2012) or lateral effects (Kelley et al. 2003). Here, rotation is suggested as a possible mechanism for reducing heat fluxes below the laboratory-derived parameterizations in some of these staircases. We discuss five examples of staircase observations, from the Arctic Ocean and tropical Lake Kivu (Carpenter and Timmermans 2012); three in which rotation is expected to be an important influence, and two in which it is not.

The first example occurs in the  $\sim 2600$ -m-deep double-diffusive staircase of the Canada Basin, Arctic Ocean. Both an approximate heat budget (Timmermans et al. 2003; Carmack et al. 2012) and an overturn analysis of the interfaces (Timmermans et al. 2003) indicate that  $F_H$  is less than that predicted using the parameterization of Kelley (1990), however, it is not known by exactly how much. Interface thicknesses within the deep staircase are generally reported to be within the range of  $2 < h < 20$  m (Timmermans et al. 2003; Carmack et al. 2012) showing that they are much thicker than  $B\delta_E = 63$  cm, based on the molecular value of  $\nu = 1.83 \times 10^{-6} \text{ m}^2 \text{ s}^{-1}$ . However, the density ratio of these interfaces is low ( $R_p \approx 1.6$  on average), raising the possibility that the heat fluxes through the interface may be turbulent (Timmermans et al. 2003; Johnson and Garrett 2004). This question was addressed in some detail by Johnson and Garrett (2004), where they concluded that overturns observed in  $T$  profiles measured with a standard CTD were indistinguishable from instrument noise. Therefore, it is possible that the interfacial fluxes in the deep Arctic staircase are close to molecular values, and that they are in the rotation-dominated regime. It is also interesting to note that we could use a turbulent eddy viscosity  $K_\nu$ , in the definition of the Ekman thickness. Timmermans et al. (2003) have estimated an eddy diffusivity for  $T$ , which we take to be equivalent to  $K_\nu$ , that is, we assume that the turbulent Prandtl number is unity (sometimes referred to as the Reynolds analogy). Based on the mean interface  $T$  gradients and an upper bound for  $F_H$ , they arrive at  $K_\nu \approx 4 \times 10^{-5} \text{ m}^2 \text{ s}^{-1}$ . Using this value of  $K_\nu$ , shows that  $B\delta_E = 3$  m, and Kelley's condition requires that  $h > 3$  m for rotation to significantly decrease heat fluxes. However, just how to define  $h$  for a turbulent interface is not clear, and we should not expect Kelley's condition to be valid in this case.

A second example of DDC interfaces that may be affected by rotation comes from the thermocline of the Laptev Sea slope region of the Arctic Ocean. Polyakov et al. (2012) report measurements of interface thicknesses that are in the range  $1 < h < 5$  m at values of  $1.5 < R_p < 3.5$ , and once again it is unclear whether the interfaces may be turbulent. Polyakov et al. (2012) have addressed this question by calculating turbulent fluxes within the interfaces of a representative DDC staircase, measured in this region by Lenn et al. (2009) with a microstructure profiler. Using the common turbulent mixing parameterization for the temperature diffusivity  $K_T = \Gamma\epsilon/N^2$ , where  $\Gamma = 0.2$  is the mixing efficiency and  $N$  is the buoyancy frequency, Polyakov et al. (2012) find  $F_H \approx 1 \text{ W m}^{-2}$  through the thick interfaces [the Kelley (1990) parameterization gives approximately 5 times larger  $F_H$ ]. Based on a mean  $T$  gradient within the

interfaces of  $\langle \partial T / \partial z \rangle = 0.0925^\circ\text{C m}^{-1}$  [see Polyakov et al. (2012), their Fig. 7], we can estimate  $K_T = F_H / \rho c_p \langle \delta T / \delta z \rangle \approx 2.4 \times 10^{-6} \text{ m}^2 \text{ s}^{-1}$ . Taking  $K_\nu = K_T$  leads to an eddy viscosity value that is only marginally larger than the molecular value, that is,  $K_\nu = 1.4\nu$ . It is also possible to calculate the buoyancy Reynolds number  $\text{Re}_b \equiv \epsilon / \nu N^2 \approx 7$ , where this low value implies that the flow is in a transitional state that is close to molecular mixing levels (Ivey et al. 2008). Taking  $\delta_E = (K_\nu / f)^{1/2}$  gives a Kelley condition of  $h > 74 \text{ cm}$ , and we conclude that rotation could be responsible for lower  $F_H$  estimates in this DDC region. It should be noted that most existing CTD measurements do not have sufficient resolution to allow us to rule out the presence of smaller staircases that may be “sandwiched” inside these larger interfaces, and this has been found to be the case in some instances. If this is the case then  $F_H$  would again be reduced from earlier estimates.

Another possible DDC staircase that could be influenced by rotation comes from the thermocline region of the Amundsen Basin (200–260-m depth). The recent temperature microstructure survey by Sirevaag and Fer (2012) in this region shows that heat fluxes, measured using two independent methods, are smaller than the Kelley (1990) parameterization by an order of magnitude. Although interface thicknesses are not reported in Sirevaag and Fer (2012), we can determine an average  $h$  through the relation  $\langle h \rangle = \rho c_p \kappa_T \langle \Delta T \rangle / \langle F_H^{\text{mol}} \rangle$ , using average values of  $\langle \Delta T \rangle = 0.062^\circ\text{C}$  (based on their Table 2 and weighted by interface number) and  $\langle F_H^{\text{mol}} \rangle = 0.05 \text{ W m}^{-2}$ . This leads to an average  $\langle h \rangle = 71 \text{ cm}$ , which is slightly greater than values of  $B\delta_E = 63 \text{ cm}$  for these latitudes. They also find close agreement between  $F_H^{\text{mol}}$  through the interfaces and  $F_H$  calculated using a mixed layer turbulence technique. This is to be expected because  $R_\rho = 3$  for this staircase on average. We therefore conclude that rotation may be responsible for the large discrepancy between the measured and parameterized  $F_H$  in the Amundsen Basin staircase.

Using the present simulations, it is difficult to make quantitative predictions of the decrease in  $F_H$  when DDC is in the rotation-dominated regime. In fact, there is considerable debate over the form of the heat transfer law in rotating thermal convection, expressed as  $\text{Nu} \propto \text{Ra}^a \text{Ek}^b$ , with various studies proposing different values of the scaling exponents  $a, b$  [see Julien et al. (2012) and King et al. (2012) for a recent discussion]. Recent studies using different boundary conditions, and in different parameter regimes have found that  $1 \lesssim a \leq 3$  and  $1.5 \lesssim b \leq 4$  (Schmitz and Tilgner 2009; King et al. 2012; Julien et al. 2012). The large value of the exponents in the heat transfer law shows that  $\text{Nu}$  is very sensitive to  $\text{Ra}$  and  $\text{Ek}$ , and  $\text{Nu}$  decreases rapidly in the rotationally dominated

regime [see also Kelley (1987)]. In the case of DDC, all that can currently be said is that  $F_H$  is strongly reduced once the Kelley condition is crossed, and it is conceivable that the discrepancy between estimated fluxes and the nonrotating parameterizations in the Arctic Ocean staircases just identified can be attributed to rotational effects.

Finally, we discuss two DDC staircases in which rotation is not expected to significantly influence heat fluxes. The shallow ( $\sim 300 \text{ m}$  deep) Canada Basin DDC staircase has been observed using a microstructure profiler by Padman and Dillon (1989) and Timmermans et al. (2008). They report that the  $T$  interfaces satisfy  $h < 40 \text{ cm}$ , indicating that rotation is not expected to significantly affect heat fluxes, because  $B\delta_E \approx 63 \text{ cm}$  at these latitudes. This conclusion is also supported by the analysis of Timmermans et al. (2008), who show that the molecular heat flux through the interfaces agrees well with the laboratory-based parameterization of Kelley (1990). It is noteworthy that the Kelley (1990) parameterization also works well in equatorial waters, and a similar analysis has been performed by Schmid et al. (2010) and Sommer et al. (2013a,b) for the DDC staircase in Lake Kivu, located at  $2^\circ\text{S}$  in tropical Africa. Once again, the microstructure-based estimates of molecular heat fluxes show good agreement with the Kelley (1990) parameterization, and the interface thickness distribution with  $h < 1 \text{ m}$ , does not approach the Kelley condition of  $B\delta_E = 2.3 \text{ m}$ .

## 5. Conclusions

In summary, we have performed the first series of experiments quantifying the effects of rotation on heat fluxes in the diffusive (semiconvection) regime of double-diffusive convection of oceanic relevance. The results support a previous theory by Kelley (1987) stating that significantly reduced heat fluxes will result when the Ekman layer thickness is sufficiently smaller than the thermal interface thickness—an idea also shown by King et al. (2009) to apply in thermal convection. The scaling law implied by this condition is applied to relevant DDC staircases in the Arctic Ocean, where we predict the possibility of significantly reduced, rotation-dominated heat fluxes in the DDC staircases of the deep Canada Basin, near the continental slope in the Laptev Sea thermocline, and in the Amundsen Basin.

*Acknowledgments.* We thank Kraig Winters for providing the DNS code and Brian Dobbins for computational support. Funding for this analysis was provided by Yale University and the National Science Foundation Office of Polar Programs under Award ARC-0806306. This work was supported in part by the Yale University

Faculty of Arts and Sciences High Performance Computing facility (and staff).

## REFERENCES

- Carmack, E., W. Williams, S. Zimmermann, and F. McLaughlin, 2012: The Arctic Ocean warms from below. *Geophys. Res. Lett.*, **39**, L07604, doi:10.1029/2012GL050890.
- Carpenter, J., and M.-L. Timmermans, 2012: Temperature steps in salty seas. *Phys. Today*, **63**, 66–67.
- , T. Sommer, and A. Wüest, 2012a: Simulations of a double-diffusive interface in the diffusive convection regime. *J. Fluid Mech.*, **711**, 411–436, doi:10.1017/jfm.2012.399.
- , —, and —, 2012b: Stability of a double-diffusive interface in the diffusive convection regime. *J. Phys. Oceanogr.*, **42**, 840–854.
- Flanagan, J., A. Lefler, and T. Radko, 2013: Heat transport through diffusive interfaces. *Geophys. Res. Lett.*, **40**, 2466–2470, doi:10.1002/grl.50440.
- Howard, S. L., J. Hyatt, and L. Padman, 2004: Mixing in the pycnocline over the western Antarctic Peninsula shelf during Southern Ocean GLOBEC. *Deep-Sea Res. II*, **51**, 1965–1979, doi:10.1016/j.dsr2.2004.08.002.
- Ivey, G., K. Winters, and J. Koseff, 2008: Density stratification, turbulence, but how much mixing? *Annu. Rev. Fluid Mech.*, **40**, 169–184.
- Johnson, H. L., and C. Garrett, 2004: Effects of noise on Thorpe scales and run lengths. *J. Phys. Oceanogr.*, **34**, 2359–2372.
- Julien, K., E. Knobloch, A. Rubio, and G. Vasil, 2012: Heat transport in low-Rossby-number Rayleigh–Bénard convection. *Phys. Rev. Lett.*, **109**, 254503, doi:10.1103/PhysRevLett.109.254503.
- Kelley, D., 1987: The influence of planetary rotation on oceanic double-diffusive fluxes. *J. Mar. Res.*, **45**, 829–841.
- , 1990: Fluxes through diffusive staircases: A new formulation. *J. Geophys. Res.*, **95**, 3365–3371.
- , H. Fernando, A. Gargett, J. Tanny, and E. Özsoy, 2003: The diffusive regime of double-diffusive convection. *Prog. Oceanogr.*, **56**, 461–481.
- King, E. M., S. Stellmach, J. Noir, U. Hansen, and J. M. Aurnou, 2009: Boundary layer control of rotating convection systems. *Nature*, **457**, 301–304, doi:10.1038/nature07647.
- , —, and J. Aurnou, 2012: Heat transfer by rapidly rotating Rayleigh–Bénard convection. *J. Fluid Mech.*, **691**, 568–582, doi:10.1017/jfm.2011.493.
- Kunnen, R. P. J., H. J. H. Clercx, and B. J. Geurts, 2006: Heat flux intensification by vortical flow localization in rotating convection. *Phys. Rev. E*, **74**, 056306, doi:10.1103/PhysRevE.74.056306.
- Lenn, Y.-D., and Coauthors, 2009: Vertical mixing at intermediate depths in the Arctic boundary current. *Geophys. Res. Lett.*, **36**, L05601, doi:10.1029/2008GL036792.
- Linden, P., and T. Shirtcliffe, 1978: The diffusive interface in double-diffusive convection. *J. Fluid Mech.*, **87**, 417–432.
- Marmorino, G., and D. Caldwell, 1976: Heat and salt transport through a diffusive thermohaline interface. *Deep-Sea Res.*, **23**, 59–67.
- Padman, L., and T. Dillon, 1987: Vertical heat fluxes through the Beaufort Sea thermohaline staircase. *J. Geophys. Res.*, **92**, 10799–10806.
- , and —, 1989: Thermal microstructure and internal waves in the Canada Basin diffusive staircase. *Deep-Sea Res.*, **36**, 531–542.
- Polyakov, I. V., A. V. Pnyushkov, R. Rember, V. V. Ivanov, Y.-D. Lenn, L. Padman, and E. Carmack, 2012: Mooring-based observations of double-diffusive staircases over the Laptev Sea slope. *J. Phys. Oceanogr.*, **42**, 95–109.
- Rosby, H. T., 1969: A study of Bénard convection with and without rotation. *J. Fluid Mech.*, **36**, 309–335.
- Schmid, M., M. Busbridge, and A. Wüest, 2010: Double-diffusive convection in Lake Kivu. *Limnol. Oceanogr.*, **55**, 225–238.
- Schmitt, R. W., 1994: Double diffusion in oceanography. *Annu. Rev. Fluid Mech.*, **26**, 255–285.
- , and R. B. Lambert, 1979: The effects of rotation on salt fingers. *J. Fluid Mech.*, **90**, 449–463.
- Schmitz, S. and A. Tilgner, 2009: Heat transport in rotating convection without Ekman layers. *Phys. Rev. E*, **80**, 015305, doi:10.1103/PhysRevE.80.015305.
- Sirevaag, A., and I. Fer, 2012: Vertical heat transfer in the Arctic Ocean: The role of double-diffusive mixing. *J. Geophys. Res.*, **117**, C07010, doi:10.1029/2012JC007910.
- Sommer, T., J. Carpenter, M. Schmid, R. G. Lueck, M. Schurter, and A. Wüest, 2013a: Interface structure and flux laws in a natural double-diffusive layering. *J. Geophys. Res.*, **118**, doi:10.1002/2013JC009166.
- , —, —, —, and A. Wüest, 2013b: Revisiting microstructure sensor responses with implications for double-diffusive fluxes. *J. Atmos. Oceanic Technol.*, **30**, 1907–1923.
- Timmermans, M.-L., C. Garrett, and E. Carmack, 2003: The thermohaline structure and evolution of the deep waters in the Canada Basin, Arctic Ocean. *Deep-Sea Res. I*, **50**, 1305–1321.
- , J. Toole, R. Krishfield, and P. Winsor, 2008: Ice-tethered profiler observations of the double-diffusive staircase in the Canada Basin thermocline. *J. Geophys. Res.*, **113**, C00A02, doi:10.1029/2008JC004829.
- Turner, J. S., 1965: The coupled turbulent transports of salt and heat across a sharp density interface. *Int. J. Heat Mass Transfer*, **8**, 759–767.
- , 2010: The melting of ice in the Arctic Ocean: The influence of double-diffusive transport of heat from below. *J. Phys. Oceanogr.*, **40**, 249–256.
- Winters, K., and E. D’Asaro, 1996: Diascalar flux and the rate of fluid mixing. *J. Fluid Mech.*, **317**, 179–193.
- , J. MacKinnon, and B. Mills, 2004: A spectral model for process studies of rotating, density-stratified flows. *J. Atmos. Oceanic Technol.*, **21**, 69–94.